NINETEENTH EUROPEAN ROTORCRAFT FORUM

Paper n° N8

COUPLED ROTOR FUSELAGE LOADS ANALYSIS- A COMPARATIVE EVALUATION AND CORRELATION

by

Mark E. Wasikowski, Michael W. Heiges, and John Bright
Research Engineers

Aerospace Laboratory
Georgia Tech Research Institute
Georgia Institute of Technology
Atlanta, Georgia USA

September 14-16, 1993
CERNOBBIO (Como)
Italy

ASSOCIAZIONE INDUSTRIE AEROSPAZIALI
ASSOCIAZIONE ITALIANA DI AERONAUTICA ED ASTRONAUTICA

COUPLED ROTOR FUSELAGE LOADS ANALYSIS- A COMPARATIVE EVALUATION AND CORRELATION

Mark E. Wasikowski, Michael W. Heiges, and John C. Bright
Research Engineers

Aerospace Laboratory
Georgia Tech Research Institute
Georgia Institute of Technology
Atlanta, Georgia USA

1. Abstract

This paper presents emerging results from an Aircraft Structural Integrity Program (ASIP) study of the H-53 helicopter. The intent of the study is the implementation of a loads assessment methodology to support structural damage tolerance analysis (DTA). Components of the study include flight testing for a loads database, experimental wind tunnel testing of the fuselage, computational fluid dynamics (CFD) modeling of the fuselage airloads, dynamic NASTRAN finite element modeling of the fuselage structure, and aircraft flight dynamics modeling with the Comprehensive Analytical Model of Rotorcraft Aerodynamics and Dynamics (CAMRAD/JA). Loads analyses are validated against experimental or flight test data.

The focus of this paper is the outline of the loads assessment methodology. The approach is to incorporate results from the experimental wind tunnel test and the dynamic NASTRAN analysis into the CAMRAD/JA model which is then used to predict applied rotor loads. The CFD model is used to predict static fuselage loads.

This paper outlines the approach and presents sample correlations of the CFD model against wind tunnel test pressure data and the dynamic NASTRAN model against shake test data. Good correlation with main rotor blade steady and vibratory loads also was observed. Including wake effects on the inflow distribution was important. Fair correlation of pilot vertical response was observed. The vibratory blade loads and fuselage response are under-predicted. Rotor - fuselage coupling is necessary to better predict fusealge vibration.

2. Introduction

Determination of critical structural loads is an important part of every helicopter design and subsequent modification. Design loads represent the starting point for the structural stress analysis and are difficult to predict accurately. Design loads include both steady and vibratory loading for critical operating conditions for primary and backup support structure. It is even more important for damage tolerance analysis (DTA) fatigue assessments wherein crack growth may take place below endurance limit loading. Although the steady load is important, the harmonic content of the vibratory loading is critical for fatigue life assessments. This study was conducted as part of an overall Aircraft Structural Integrity Program (ASIP) by Georgia Tech and Sikorsky Aircraft for the U.S. Government, Ref. 1. The program's intent is to improve design, diagnose possible structural failures, give a basis for corrective action, and predict operational inspection intervals and life expectancy of rotorrcraft.

Presented at the 19th European Rotorcraft Forum, September 14-16, 1993, CERNOBBIO (Como), Italy.

The goal of this study is to enhance the damage tolerance techniques that are being applied to the H-53 helicopter

Figure 1 shows the various components of the overall ASIP study. Currently the study is focused on the loads spectrum database generation presented in the lower left portion of Figure 1. The overall objectives are to provide a spectrum of H-53 rotor and fuselage structural loads applied to selected components for DTA analysis. This consists of both steady and vibratory loading during steady state and transient maneuver flight conditions for arbitrary vehicle payload configurations and flight conditions. The pieces of this approach are illustrated in Figure 2. The loads database for the spectrum consists primarily of flight test data. This is supplemented with empirical curve fitting of the test data and analytical predictions. Flight test loads are statistically analyzed and used for building a database for DTA analysis and validation of supplemental analysis. Analytical loads predictions are provided through flight dynamics and structural finite element analysis. The overall procedure for loads estimation is to correlate structural loads from their origin as aerodynamic and inertial loads on the main and tail rotor blades, empennage, and fuselage with existing flight test data

Other approaches for estimating coupled rotor/fuselage dynamics were investigated in the Design Analysis Methods for Vibrations (DAMVIBS) program, Ref. 2 and 3. These analysis focused on the dynamic coupling at the rotor hub. Rotor and fuselage coupling is obtained by requiring compatible loads and displacements at the main and tail rotor hub.

Fuselage airloads are then calculated using a VSAERO, Refs. 3,4, computational fluid dynamics (CFD) panel model. The forces, moments, and pressures are compared to wind tunnel test results for validation. The VSAERO model is then used to determine static load distributions on the airframe. The wind tunnel test also provides the fuselage aerodynamic characteristics for the flight dynamics analysis. The fuselage structural loads analysis is accomplished using dynamic NASTRAN, Ref. 5. CAMRAD/JA (Comprehensive Analytical Model of Rotorcraft Aerodynamics and Dynamics), Ref. 6 is used for a coupled rotor/body loads assessment. CAMRAD/JA has been used in other loads assessments and correlations, Refs. 7-10. The NASTRAN structural finite element model is used to provide normal modes and hub motions to CAMRAD/JA. Local steady and vibratory loads on the airframe are determined by NASTRAN given the CAMRAD/JA applied rotor airloads and VSAERO fuselage airloads. The final step consists of validating the loads analysis methods against experimental data from the loads survey database.

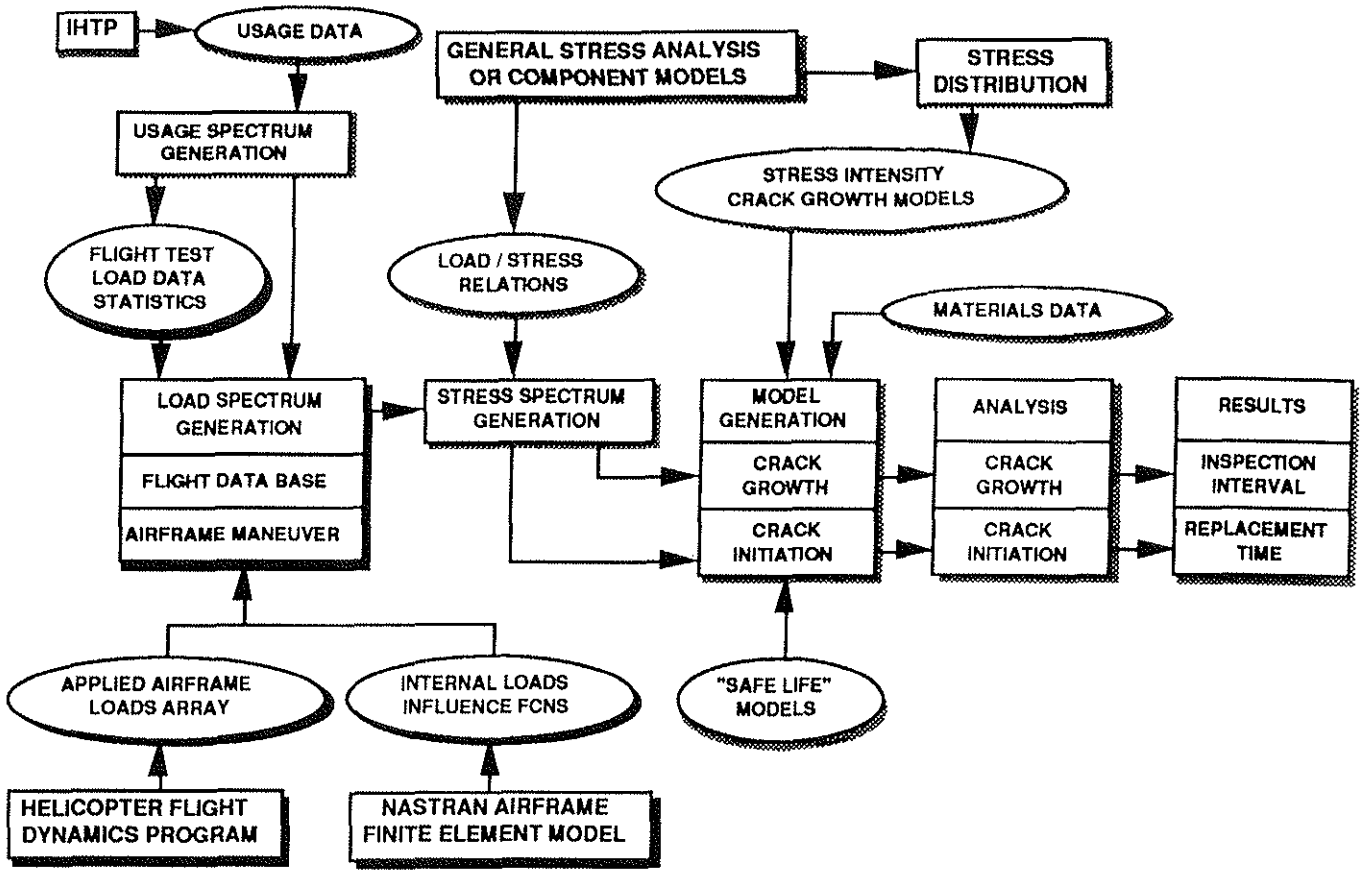

Figure 1. Damage Tolerance Analysis Program

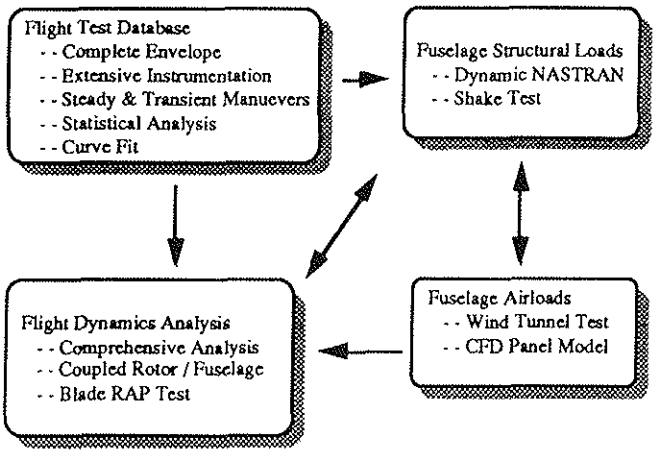

Figure 2: ASIP DTA Loads Assessment Components

3. Flight Test Program

An H-53 helicopter is being flight tested as part of an airworthiness qualification program for the U.S. Government. The flight program consists of a structural flight strain and vibration survey, Automatic Flight Control System (AFCS) collective optimization study, high altitude evaluation, flight performance and range optimization, and simulator validation phases. Currently, the shakedown, developmental flight testing, preliminary flight strain survey, and AFCS optimization portions have been completed. Results herein are based on this preliminary flight strain survey. A final flight strain and loads survey will consist of additional strain parameters and flight conditions to complete the fatigue spectrum flight conditions.

The general aircraft configuration, Figure 3, is a six bladed single main lifting rotor helicopter with a four bladed anti-torque tail rotor and twin T64-GE series turboshaft engines. The main rotor is fully articulated with an elastomeric bearing and a wide chord titanium spar blade referred to as the Improved Rotor Blade (IRB).

A lag damper resists the lead-lag motion of the blade, while the elastomeric rotor head resists flapping motion. The blade has coincident flap and lag hinges, a nonlinear twist distribution, a SC1095 airfoil section, and a swept and tapered blade tip.

Flight test conditions flown include over 20 specific combinations of gross weight, center of gravity, rotor speed, and altitude. These included advance ratios from zero to 0.36, rotor speeds at 100% and 105% of the nominal design value, thrust coefficient/solidity ratios from 0.06 to 0.13, and centers of gravity (CG) ranges from the full forward to the full aft qualified limit with some midrange CG's. For each configuration, a level flight speed sweep was performed, as well as steady and transient maneuvers associated with a defined usage spectrum for fatigue life assessments. These flight conditions encompass the effects of blade stall, CG location, rotor speed, and airspeed on the steady and transient dynamic response and loads on selected dynamic components and fuselage structure. Steady level flight speed sweeps were selected here for correlation purposes.

Flight test instrumentation included over 55 flight parameters recorded on Pulse Code Modulation (PCM) tape, 235 strain gauge and vibration parameters recorded on Frequency Modulation (FM) and Digital Audio Tape (DAT) tapes, and 56 AFCS parameters on PCM tape. Main rotor measurements included shaft bending and torque, stationary swashplate and servo loads, swashplate guide moments, stationary and rotating scissors bending

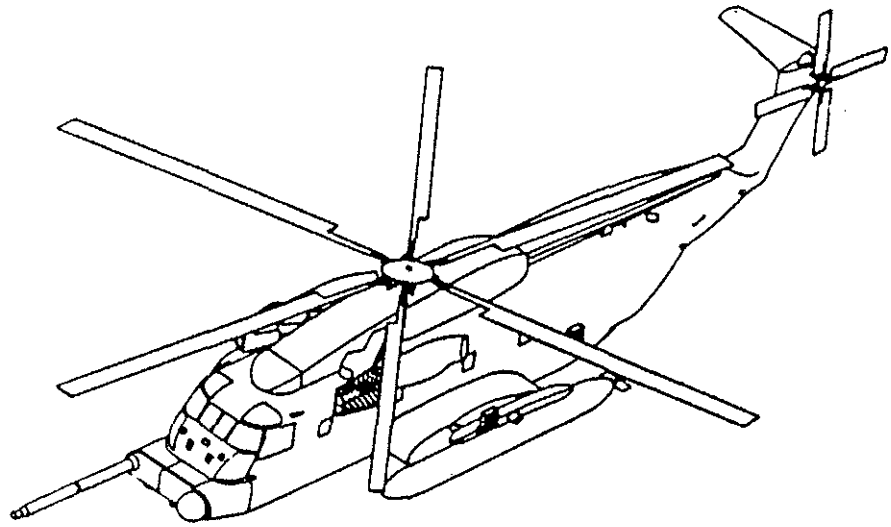

Figure 3. Flight Test Aircraft

moments, pitch link axial load and bending moments, damper rod end axial load and bending moments, blade flapping and edgewise bending at the various radial stations and at the elastomeric bearing assemblies. Flapping and coning were derived from the shaft bending measurements. Tail rotor measurements included the pylon shaft, output shaft, blade, spindles, and pitch beam bending loads, as well as the flapping, and impressed pitch. Fixed system measurements included landing gear loads, engine and cockpit vibration, and strain and vibrations at various other locations on the fuselage and empennage.

4. Flight Test Loads Database

The primary source for loads data for DTA analysis is a strain, stress, and vibration database derived from the flight test. The objective of the database is to provide structural loads for crack propagation analysis and data for analytical model validation. Data processing methods used are the peak stress scanning technique, rainflow cycle counting, and harmonic analysis, based on the techniques described in Ref. 11.

Peak stress scanning of the time histories involves digitizing the analog flight test data at a single frequency, usually the dominant frequency. During each cycle, the minimum and maximum values are used to determine the steady and vibratory stress levels. This method is more accurate for data wherein one frequency dominates the response. It is less accurate for more complex waveforms where multiple frequencies are significant, such as those driven by significant blade stall and blade vortex interactions. However, it is computationally efficient.

Rainflow cycle counting is a more realistic estimate of the damage causing loading cycles based on their frequency content. Harmonic analysis of the loads data provides an accurate estimate of the frequency content; however, additional processing is required for counting the number of damaging cycles.

5. Wind Tunnel Testing

A 1/25th scale model of the H-53 fuselage (see Figure 4) was tested in the GTRI Model Test Facility (MTF) to determine fuselage aerodynamic characteristics. The model was constructed from mahogany wood with the use of a numerically controlled (NC) machine. The skin contours were obtained from the NASTRAN skin element grid points. Measured parameters included the three axes forces and moments and pressure differentials at 100 locations on the body.

The test fixture allowed the model to be swept from -10° to 16° angle of attack and from 0° to 25° angle of sideslip. The model had removable components including the rotor hub, empennage, sponsons, nacelles, and external fuel tanks. In addition, the rear loading cargo door could be tested in the open or closed position.

The first objective of the wind tunnel test was to determine the effects of component changes on the H-53 airloads. Scale effects were examined. Reynolds number effects were adequately accounted for by using grit strips on the model to induce turbulent flow. This was verified by comparisons to previous wind tunnel testing of a 1/5 scale model of a slightly different configuration. The fuselage force and moment characteristics with angle of attack and sideslip were then determined and are being used in the flight dynamics assessment.

The second objective of the test was to determine the pressure distribution over the fuselage for local applied airloads. One hundred pressure taps were located along the upper and lower surface centerline, along the left and right side middle waterline, and in a ring about a station line just aft of the cockpit section. The pressure distribution data is being used to validate a VSAERO computational fluid dynamic model of the fuselage as described in the next section.

6. Fuselage Airloads

Fuselage pressure airloads are estimated using the computational fliud dynamics program, VSAERO. The fuselage external geometry is modeled as quadrilateral panels. A surface singularity panel method is employed by distributing doublet and source singularities in piece wise constant form on the surface panels. The panel source strengths are determined from boundary conditions controlling the normal component of the local resultant flow. The doublet strengths are determined by imposing the zero perturbation potential internal boundary conditions at all the panels simultaneously. Surface perturbation velocities are obtained from the gradient of the doublet solution. The H-53 surface panel geometry is

shown in Figure 5. The fuselage panel geometry was obtained from the NASTRAN skin grid points. This ensures compatibility with the pressure transducer locations on the wind tunnel model.

The purpose of paneling the exterior skin geometry using a potential approach is twofold. The first purpose is to provide local pressure airloads to NASTRAN for structural analysis and forced response. The second is to examine the effects of rotor/fuselage interference. An example correlation of the VSAERO surface pressure results with the wind tunnel test results is shown in Figure 6. Overall, the qualitative trend in the correlation is good. Analysis pressure spikes near the nose section are attributed to inadequate grid size. Ongoing work continues to refine the nose panel section to a finer grid size.

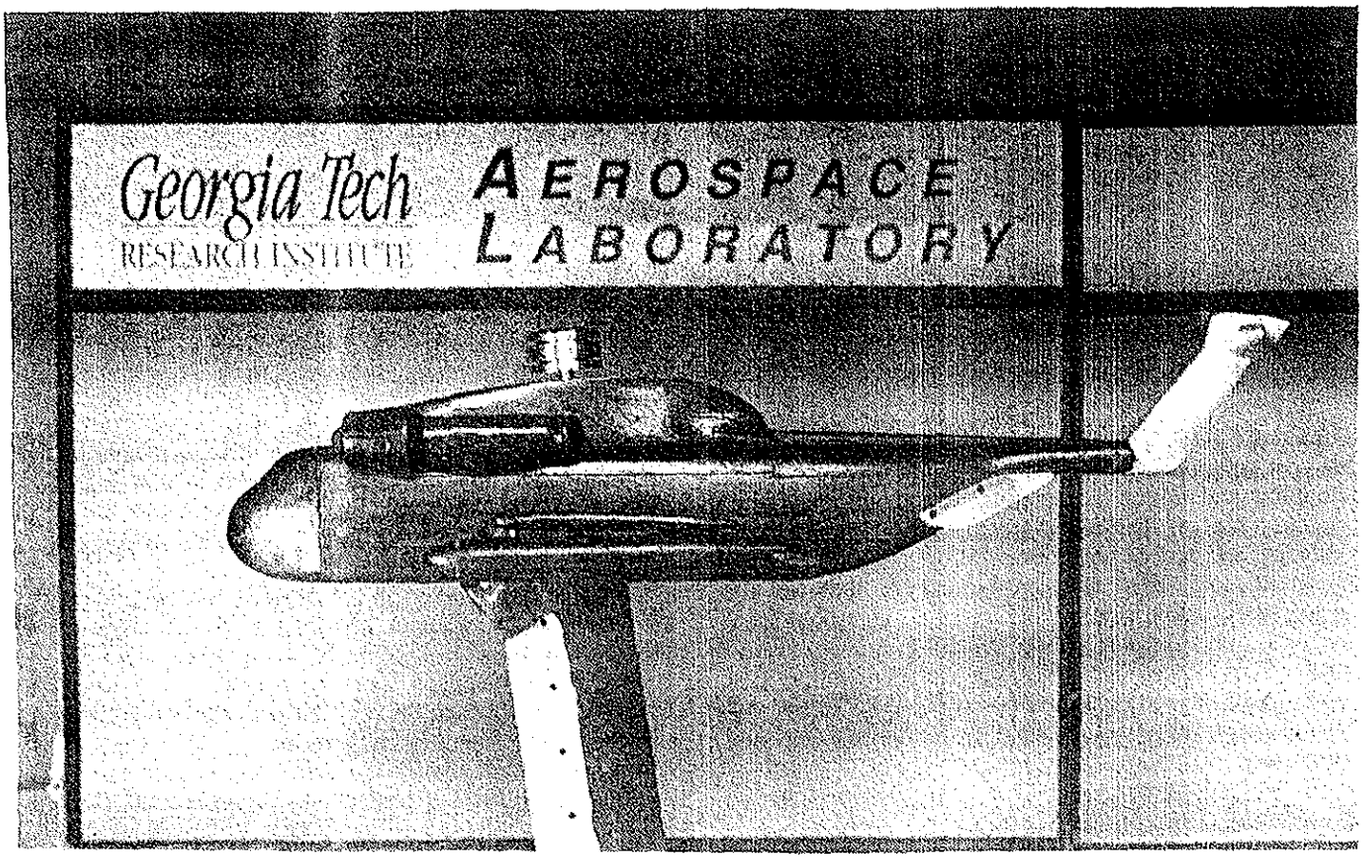

Figure 4: Wind Tunnel Test Model

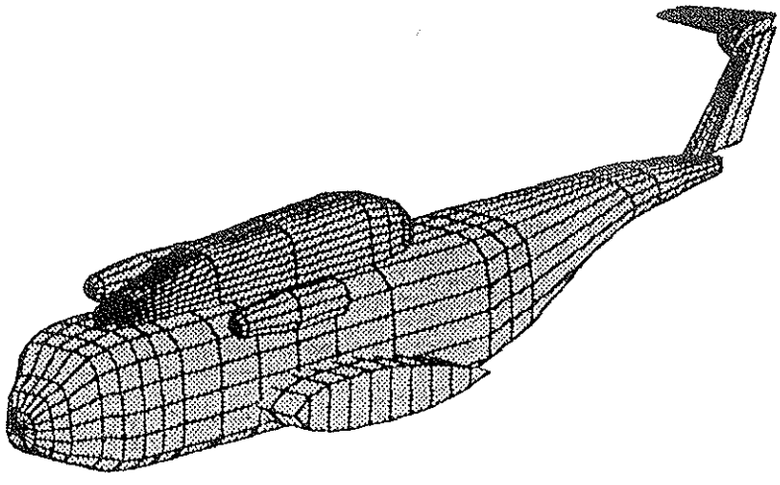

Figure 5: VSAERO Grid Model

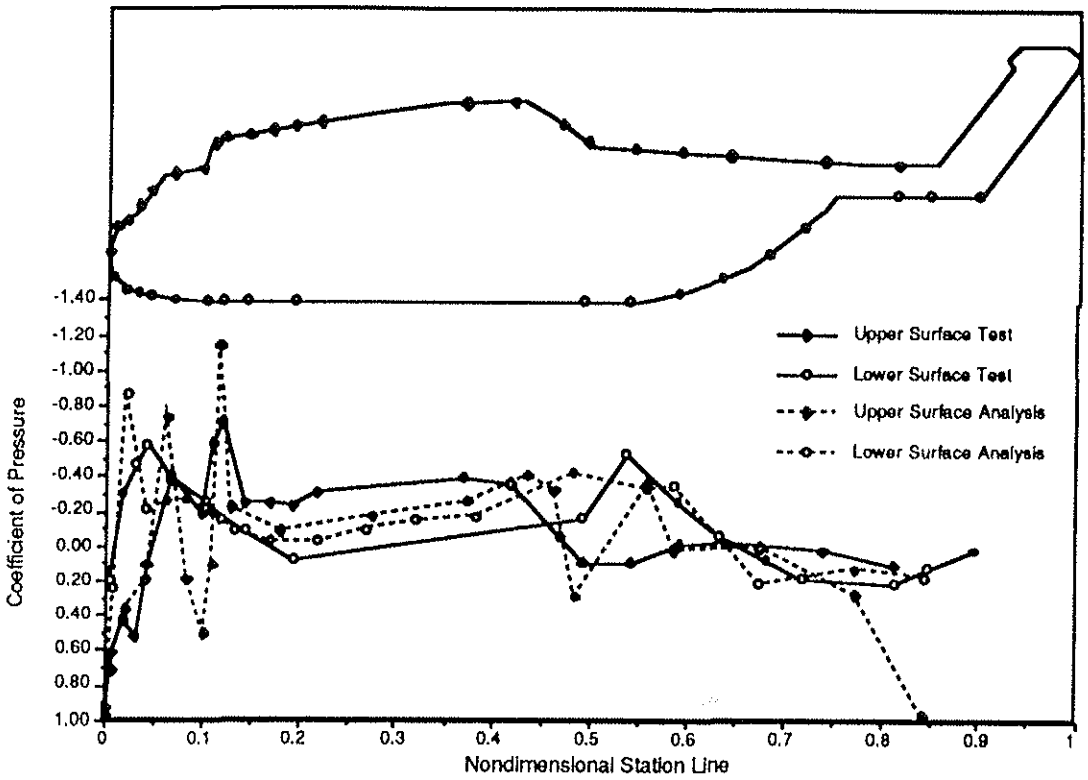

Figure 6: Comparison of VSAERO and Wind Tunnel Test

7. NASTRAN Modeling

The fuselage structural loads analysis component of the ASIP study is being conducted with MSC/NASTRAN,Ref. 5. MSC/NASTRAN uses a finite number of structure elements to represent the distributed physical properties of the structure. The elements are interconnected at a finite number of grid points to which loads are applied and for which displacements are calculated. NASTRAN modeling provides normal modes for fuselage vibration analysis. The VSAERO and CAMRAD/JA analysis provide applied loads to NASTRAN for local structural loads calculations. The NASTRAN model is then used to predict loads at locations where no instrumentation existed on the flight test and for different aircraft configurations, centers of gravity, gross weights, auxiliary equipment distribution, etc. where flight test data was not taken.

The baseline H-53 NASTRAN model shown in Figure 7 contained 4936 GRIDs, 148 CQUAD4, 2375 CBAR, 296 CTRIA3, 3986 CSHEAR, 6539 CONROD, and 280 CONM2 elements. Construction of a dynamic NASTRAN model from the static one involved developing mass, stiffness, and damping properties of the elements and the complete helicopter. In the static model, skin panels were CSHEAR elements which carry the in-plane shear loads. These elements are surrounded by CONROD elements representing the stringers plus an "effective skin" area, which carry only axial loads. This assumed that all skin panels are post-buckled and forces all the longitudinal load into the stringers. A modification was made for dynamic analysis. The skin panels were modeled using CQUAD4 elements with membrane properties only (no out of plane bending) rather than CSHEAR. The helicopter fuselage can be thought of as a reinforced thin-walled tube. There are no longitudinal beams which carry a large percentage of the loading.

It was apparent that leaving out the skin's tension and compression carrying capability greatly reduces the effective area of the tube wall making it too compliant. Using CQUAD4 elements instead of CSHEAR elements enables the skin to carry in-plane tension and compression as well as shear. With this modification the "effective skin" area was deleted from the CONROD area to prevent over-stiffening the model. The first vertical bending mode prediciton increased from 2.8 to 3.6 HZ. A first vertical bending mode frequency of 3.7 to 3.8 HZ was identified in flight test, which more closely matched the model prediction of 3.6 using CQUAD4 elements for the skin panels.

The dynamic model is being correlated against vibration results from a dynamic ground shake test, Ref. 12. The shake tests were performed by suspending the aircraft from a simulated main rotor head by using a soft bungee suspension system. In addition, a soft bungee system was used at the tail to control the attitude of the aircraft. The aircraft was dynamically excited by using a unidirectional shaker that can apply sinusoidal forces in one of the three directions at a time (vertical, lateral, and longitudinal). The shaker was mounted on the simulated rotor head. Frequency sweeps were made for strain gages and accelerometers placed at selected locations and the amplitude and phase of the response were obtained. The frequency range was from 200 to 1,700 cycles per minute (CPM).

Figures 8 and 9 are examples of the correlation between the dynamic NASTRAN model and the shake test for the vertical acceleration at the pilot's seat due to a longitudinal and vertical excitation, respectively.

The first vertical bending mode of the fuselage is slightly over-predicted, despite the improvement made by replacing the skin panels as discussed earlier. The transmission pitch mode is captured in the longitudinal response, although the magnitude is under-predicted. The transmission pitch mode is also evident in the vertical

response where no mode was obtained in the shake test. The second vertical and third coupled lateral/vertical mode resonance correlation is fair and the magnitude is under-predicted. Although the first few modes have improved correlation, it is evident further refinement is necessary to adequately model the dynamic response of the structure. Additional modeling underway includes the canopy, secondary structure, and refining the mass distribution of the fuselage structure.

The elastic fuselage modes from the dynamic NASTRAN model have been incorporated into the flight dynamics model discussed in the next section. These include the elastic lateral, vertical, and longitudinal modes of the fuselage including transmission pitching motion. Modal participation at the pilot's seat, main rotor hub, and tail rotor hub is used.

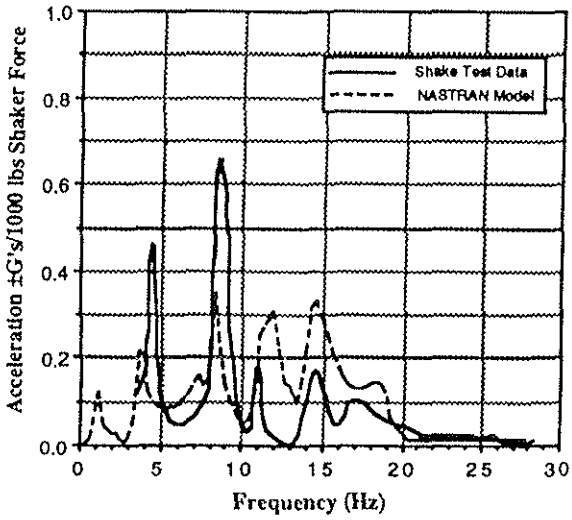

Figure 8: Pilot Vert Response to Long Acceleration

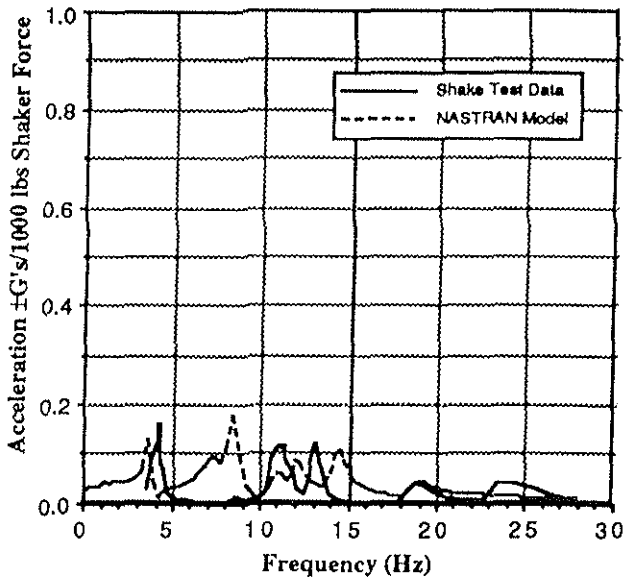

Figure 9: Pilot Vert Response to Vert Acceleration

8. Flight Dynamic Analysis

A flight dynamics assessment was conducted to integrate the various portions of the DTA loads effort together to provide global coupled rotor / fuselage loads. CAMRAD/JA was used for this purpose. CAMRAD/JA is a comprehensive analysis for calculating rotor dynamics and performance, aerodynamic and structural loads, aircraft vibration and gust response, flight dynamics, handling qualities, acoustics, and system aeroelastic stability.

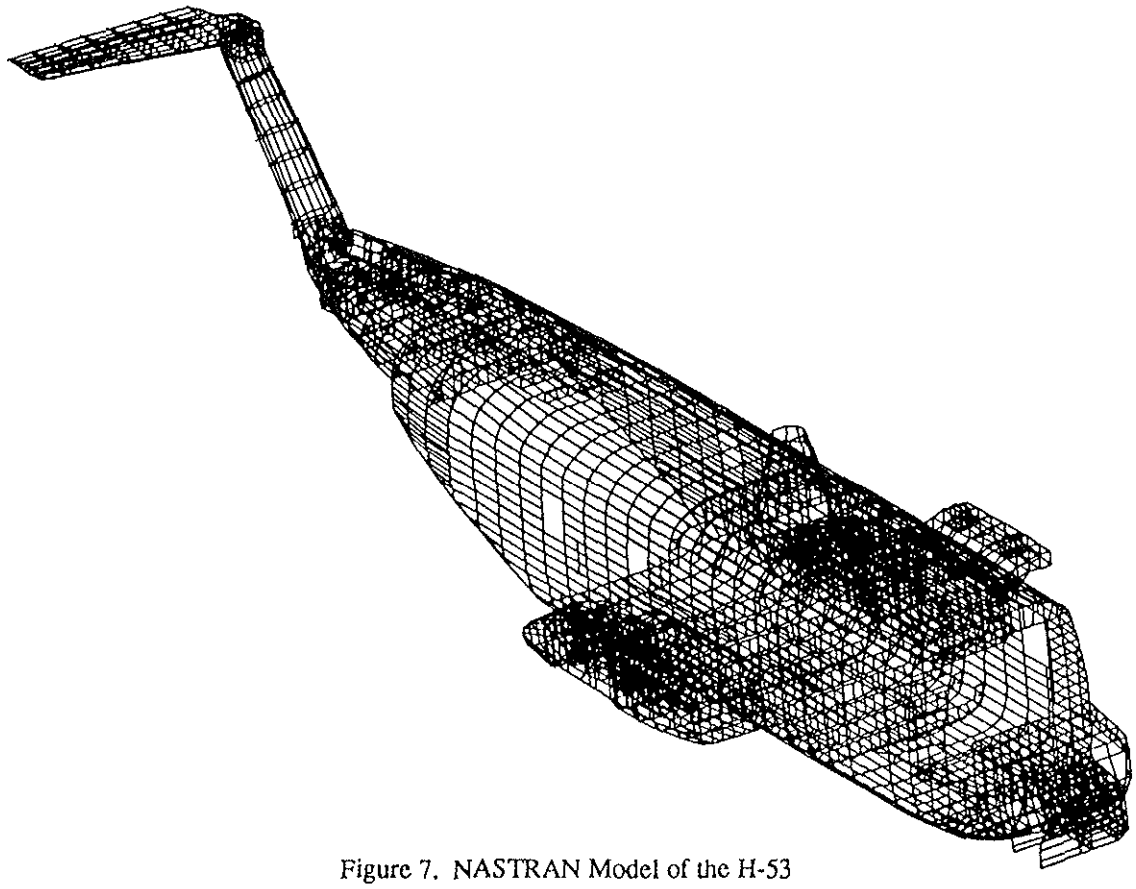
Figure 7. NASTRAN Model of the H-53

A summary of the various aerodynamic and structural modeling assumptions and options is discussed in Ref. 6. The structural representation of the blade is based on engineering beam theory for rotating wings with large pitch and twist. The blade motion is described by rotating free-vibration modes equivalent to a Galerkin analysis. The aerodynamic model consists of lifting-line airloads using steady two-dimensional airfoil characteristics. Inflow is obtained from either a Coleman momentum theory model, a prescribed vortex wake, or free vortex wake. Empirical dynamic stall, yawed flow, and unsteady thin airfoil aerodynamic effects are also modeled.

The H-53 is modeled as a single main rotor and anti-torque rotor attached to a fuselage. The main rotor was modeled as a hinged articulated hub with elastic blades. An effective flap hinge spring is included due to the elastomeric bearing. Nonlinear lag damper characteristics are included from the hub geometry and damper bench tests. The blade has 25 aerodynamic segments and 49 structural stations. The wake is modeled as either uniform momentum or vortex based on prescribed or free wake geometries. Aircraft geometry and inertial properties were obtained from drawings, Sikorsky Engineering Reports (SER's), and measurements of the flight test aircraft. Fuselage flexibility was modeled using normal modes from the NASTRAN analysis. Fuselage aerodynamic properties were obtained from the wind tunnel test discussed previously.

Free flight trim sweeps were performed using two methods. First, a propulsive trim was used which trimmed the overall aircraft forces and moments using the pilot's controls and vehicle attitudes. Degrees of freedom for this trim included the 6 fuselage rigid body modes, fuselage normal vibration modes, main rotor flap, lag, and torsional rigid and elastic modes, and tail rotor rigid flapping. The second method was a wind tunnel trim of the main rotor to the thrust, power and flapping angles obtained from the flight. Flapping was derived from main rotor shaft bending.

Fuselage pitch attitude is compared to the flight test data in Figure 10 for flight 57, a 46,000 LB gross weight forward center of gravity position. Three different wake models were used. These were the uniform (linear variation), prescribed, and free wakes. The uniform inflow under-predicts the fuselage pitch attitude, whereas both the wake models obtain a reasonable trim as compared to the test data, except for very low speed. Main rotor power is compared to flight test data for the same conditions in Figure 11 using the different wake models. The free wake analysis tends to over-predict the power through transition and under-predict the power at higher airspeeds.

The uncoupled rotating IRB main rotor blade frequencies are presented in Figure 12 versus rotor speed for zero collective pitch. CAMRAD/JA is compared to a 24 lumped mass Myklestad analysis, Ref. 13. Overall, the correlation is good. However, higher frequency modes are slightly over-predicted. Rigid pitch is also included based on equivalent control system stiffness. Test data comparisons were limited. IRB whirl stand data which used frequency excitation techniques demonstrated flapwise resonances at 3P and 5P which is in general agreement with both CAMRAD/JA and Myklestad analysis. However, the results were limited due to the lag damper excitation magnitude relative to the input force and the location of the strain gauges relative to the anti-nodes. A rapid applied pulse (RAP) test of the blades is underway to determine the coupled nonrotating frequencies experimentally.

The blade steady flapwise bending moment at the 0.48% radius station is presented in Figure 13 for flight 57. Both the propulsive and wind tunnel trim provide approximately the same results. The different wake models were also investigated. The prescribed wake model provided the best results for low speed flight. The steady moment was slightly under-predicted for all airspeeds.

The blade steady edgewise bending moment at the 0.48% radial location is presented in Figure 14 for the three wake models. Uniform inflow under-predicts the steady edgewise bending. Both the other inflow models under-predict the load at lower speed and over-predict at higher speed, although the overall correlation is good.

The vibratory edgewise bending at the 0.48% radial station is presented in Figure 15. Here, all the wake models under-predict the vibratory load, especially at lower airspeeds. The free wake performs significantly better than either prescribed wake or uniform inflow, however.

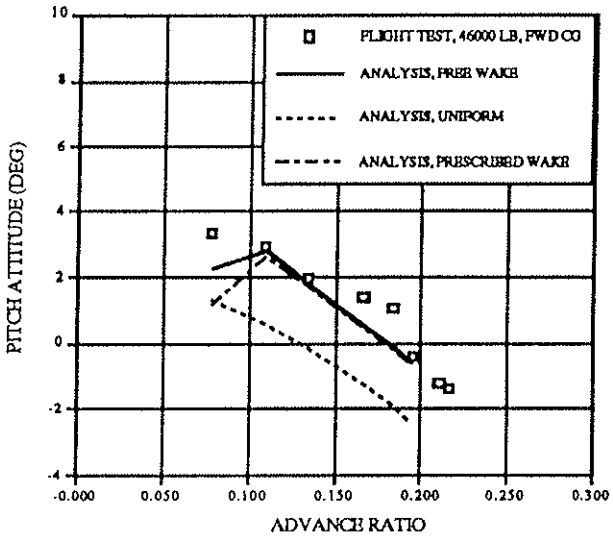

Figure 10 Fuselage Pitch Attitude Versus Advance Ratio

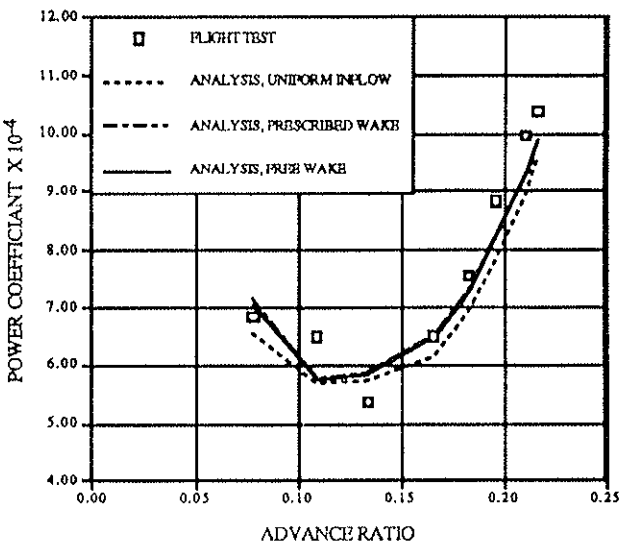

Figure 11. Main Rotor Power Versus Advance Ratio

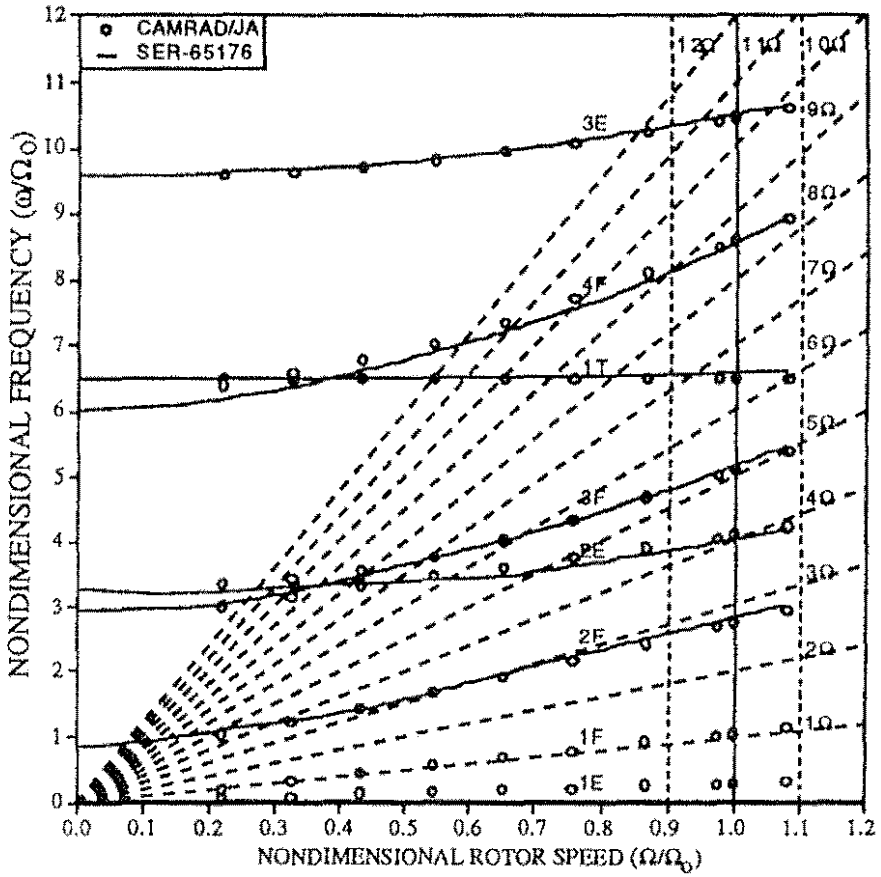

Figure 12. IRB Main Rotor Blade Frequencies

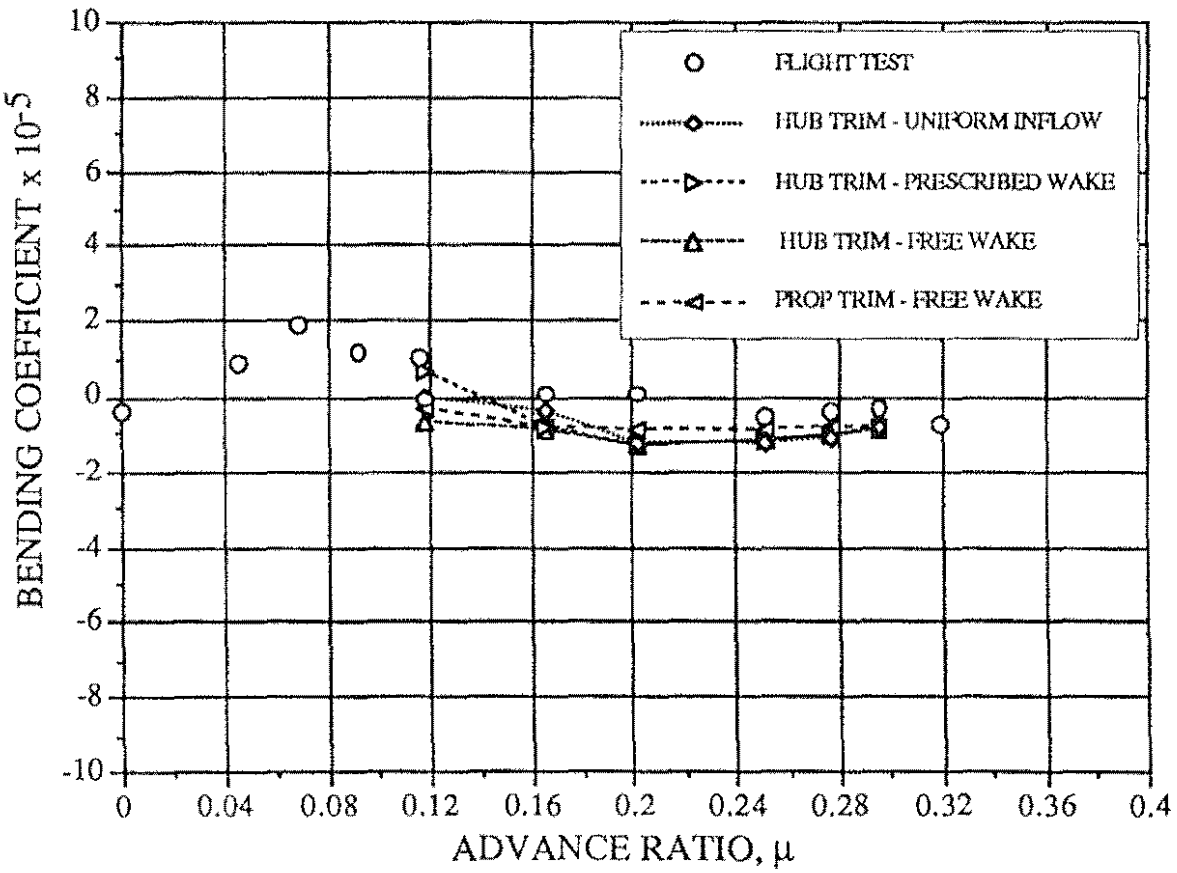

Figure 13. Steady Flapwise Bending Moment at 0.48 % Radius

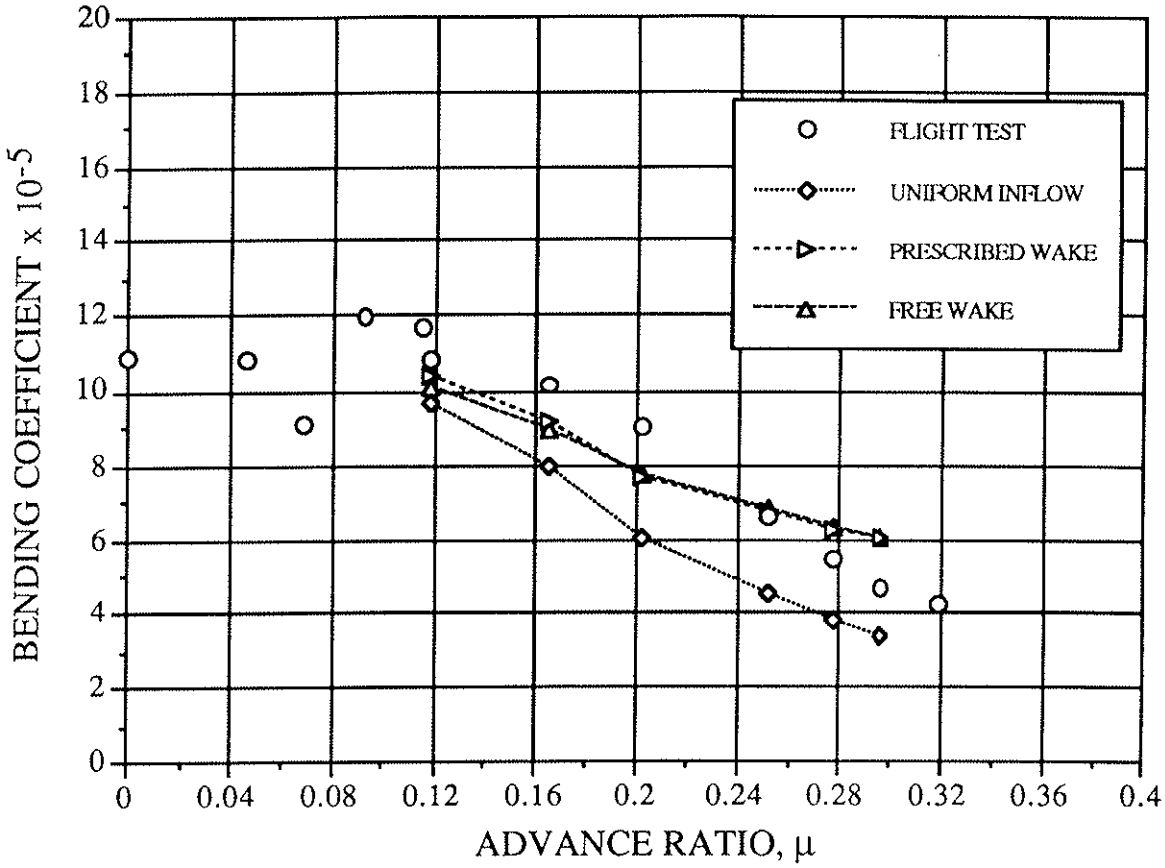

Figure 14. Steady Edgewise Bending Moment at 0.48 % Radius

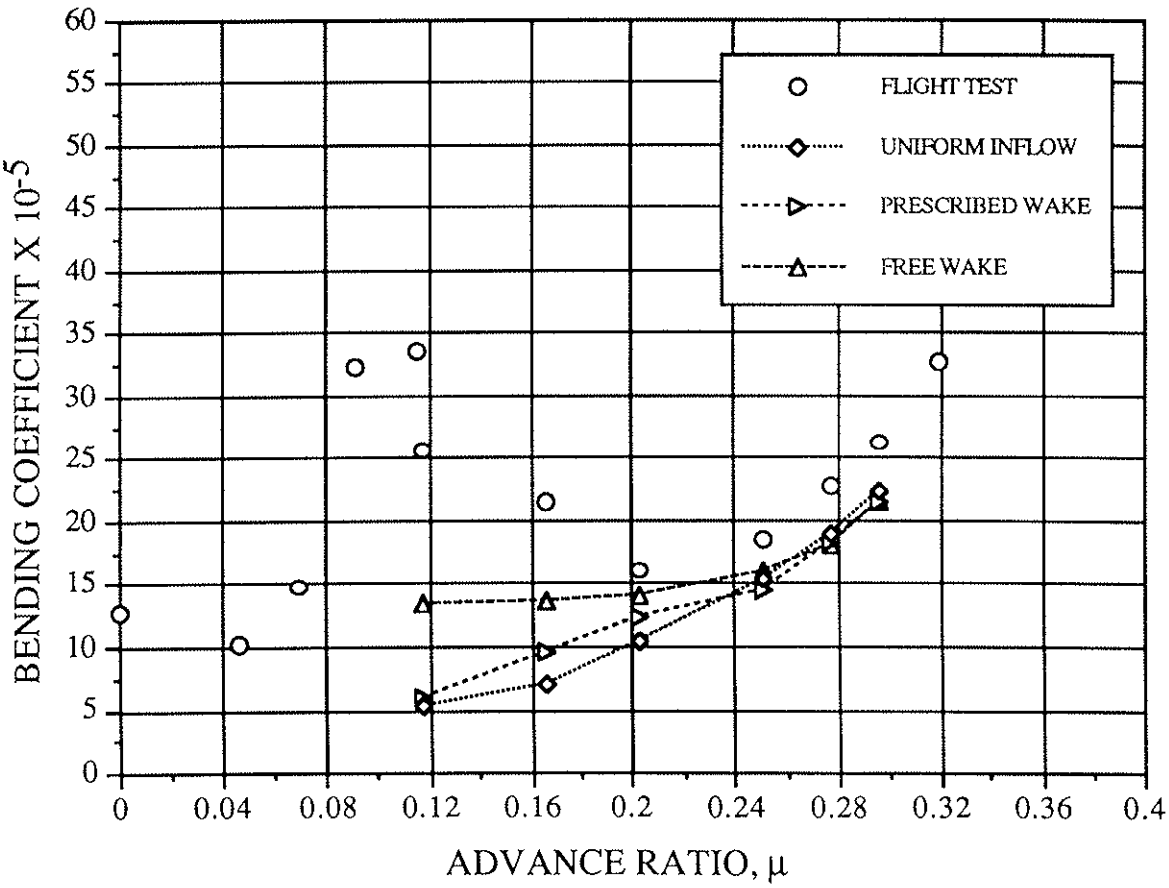

Figure 15. Vibratory Flapwise Bending Moment at 0.48 % Radius

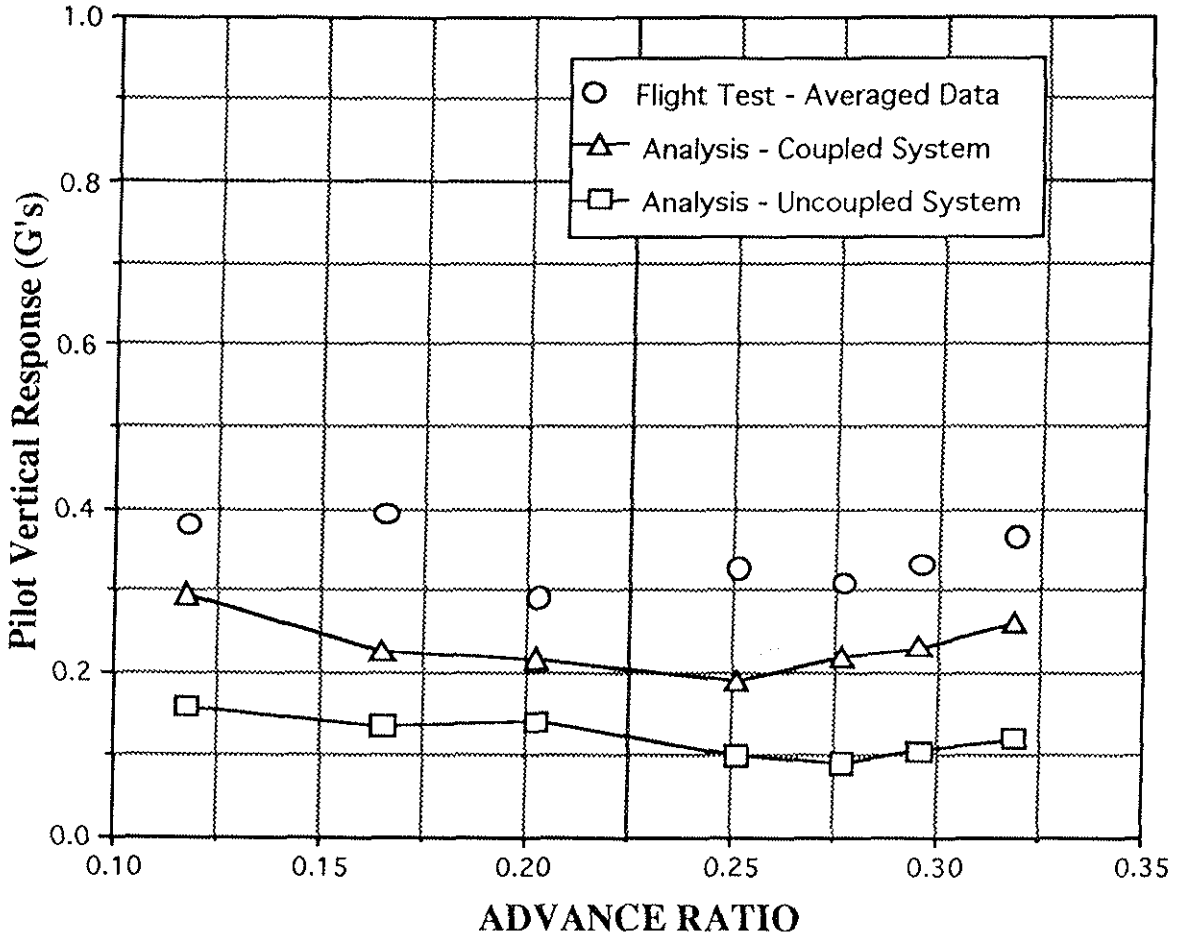

Figure 16.

9. Summary

This paper presented emerging results from an Aircraft Structural Integrity Program (ASIP) study of damage tolerance analysis (DTA) techniques applied to the H-53 helicopter. Analysis components of the study included fuselage computational fluid modeling, dynamic NASTRAN modeling of the fuselage structure, and aircraft flight dynamics analysis using a coupled rotor / fuselage program. Experimental components of the study included flight testing, wind tunnel testing, and blade RAP testing. Each portion of the program has been correlated with either experimental or flight test data. The loads obtained from the flight test and analysis will be used to form a loads spectrum database for further DTA analysis.

The wind tunnel test results correlated well with previous test results and pressure distributions produced fair correlation with CFD modeling. NASTRAN structural modeling of the fuselage produced fair correlation with shake test data. Flight dynamics modeling utilizing wind tunnel test results yielded good estimates of aircraft trimmed position and power for steady level flight conditions. Good correlation with main rotor blade steady and vibratory loads also was observed. Including wake effects on the inflow distribution was important. Fair correlation of pilot vertical response was observed. The vibratory blade loads and fuselage response are under-predicted. Rotor - fuselage coupling is necessary to better predict fusealge vibration.

10. Acknowledgement

This work was supported, in part, under U.S. Government Contract. The technical monitor is Mr. G. Chamberlain. The authors also wish to acknowledge Mr. Steve Turney and Mr. Kurt Niebur, student assistants, for their support.

11. References

1. P. Bates, C. C. Crawford, G. Chamberlain, Recent Developments in Damage Tolerance Analysis for Helicopters, Paper n^{o} N3, Nineteenth European Rotorcraft Forum, CERNOBBIO (Como) Italy, 14-16 Sept., 1993.
2. R.A. DiTaranto and V. Sankewitsch, Calculation of Flight Vibration Levels of the AH-1G Helicopter and Correlation with Existing Flight Vibration Measurements, NASA CR-181923.
3. J.D. Cronkite, R.V. Dompka, J.P. Rogers, J.C. Corrigan, K.S. Perry, and S.G. Sadler, Coupled Rotor / Fuselage Dynamic Analysis of the AH-1G Helicopter and Correlation with Flight Vibration Data, NASA CR-181723.
3. D. Clark, Study For Prediction of Rotor/Wake Fuselage Interference, Part I, Theory Manual, NASA CR-16653.
4. PROGRAM VSAERO, A Computer Program for Calculating the Non-linear Aerodynamic Characteristics of Arbitrary Configurations, NASA CR 166716.
5. M. Gockel, MSC/NASTRAN Handbook for Dynamic Analysis, MacNeal-Schwnedler Corp., June 1983.

6. W. Johnson, A Comprehensive Analytical Model of Rotorcraft Aerodynamics and Dynamics, Volume I, Theory Manual, Johnson Aeronautics, 1988.
7. G.K. Yamauchi, R.M. Heffernan, and M. Gaubert, Correlation of SA349/2 Helicopter Flight Test Data with a Comprehensive Rotorcraft Model, Journal of the American Helicopter Society, April, 1988, pp. 31-42.
8. C. Young, W.G. Bousman, T.H. Maier, F. Toulmay, and N. Gilbert, Lifting Line Predictions for a Swept Tip Rotor Blade, presented at the American Helicopter Society 47th Annual Forum and Technology Display, Phoenix, AZ, May 6-8, 1991, pp. 1345-1370.
9. W.G. Bousman and T.H. Maier, An Investigation of Helicopter Rotor Blade Flap Vibratory Loads, presented at the 48th Annual Forum of the American Helicopter Society, Washington, D.C., June 1992, pp. 977-999.
10. B.H. Lau, A.W. Louie, C.P. Sotiriou and N. Griffiths, Correlation of the Lynx-XZ170 Flight-Test Results Up to and Beyond the Stall Boundary, presented at the American Helicopter Society 49th Annual Forum, St. Louis, MO, May 19-21, 1993, pp. 1235-1253.
11. W. Fujimoto, H-53 Damage Tolerance Assessment Flight Data Rainflow Cycle Count Processor - Final Report, SER-651458, Sikorsky Aircraft, Dec. 1992.
12. P.D. Dripchak, HH-53C Ground Shake Test Report, Sikorsky SER-65651, Sikorsky Aircraft, Dec. 16, 1968.
13. M.A. Gockel, Structural Dynamic Analysis Report, Sikorsky SER-65176, Sikorsky Aircraft, June 23, 1964.